Efficient $K\alpha$ x-ray source from femtosecond laser-produced plasmas

A. Rousse, P. Audebert, J. P. Geindre, F. Falliès, and J. C. Gauthier
Laboratoire pour l'Utilisation des Lasers Intenses, Ecole Polytechnique, 91128 Palaiseau, France

A. Mysyrowicz, G. Grillon, and A. Antonetti
Laboratoire d'Optique Appliquée, Batterie de l'Yvette, Ecole Nationale Supérieure des Techniques Avancées, 91120 Palaiseau, France

(Received 8 March 1994)

We have performed a detailed quantitative study of the intense electron pulse produced by nonlinear absorption during ultrafast laser-solid interaction at near normal incidence. The resulting $K\alpha$ x-ray lines have been investigated by time-integrated spectroscopy in the 1–4 keV range and by Monte Carlo simulations of hot electron energy penetration in Al-SiO_2 and Al-CaF_2 targets. Calibration of the observed electron fluence and $K\alpha$ line intensities was provided by direct monoenergetic electron beam interaction with the same target. Optimum conditions for hot electron production were obtained by setting the prepulse energy fluence close to the target damage threshold. Results indicate that $K\alpha$ lines were produced by a distribution function of hot electrons which carry 12% of the incident laser energy with a characteristic temperature of about 8 keV. Spectrally and spatially resolved $K\alpha$ emission measurements using a cooled charge-coupled-device detector demonstrate the scaling capabilities of this x-ray source to energies in excess of 6 keV.

PACS number(s): 52.50.Jm, 52.40.Nk, 52.70.La, 32.30.Rj

I. INTRODUCTION

The generation of ultrabright and ultrafast x-ray pulses is a challenge in the study of unexplored physics of high density and high temperature plasmas [1]. Such plasmas are produced when an intense ultrashort laser pulse (100 fs, 10^{16-17} W/cm^2) is focused on solid targets [2–9]. Laser energy absorbed within the laser skin depth [10,11] gives rise to a thermal plasma of several hundred electron volts temperature, approaching solid density [12,13]. Very short x-ray emission from the thermal plasma is expected within this short time scale because electrons cannot transfer a significant fraction of their energy to ions and very weak expansion occurs during the pulse [14–16]. Behind the thermal plasma, fast electrons resulting from the specific interaction of the incident laser light through a very steep density gradient—with a scale length being only a fraction of the incident laser wavelength [17–20]—eject inner shell electrons of the target plasma. This produces fluorescence line radiation as the inner shell vacancy is filled from outer shells [7,21–23].

Most of our knowledge of the physics of laser plasmas in the $I\lambda^2 > 10^{14}$ (W/cm^2)μm^2 regime (where I is the laser irradiance and λ its wavelength) comes from the work done with CO_2 and Nd:glass lasers 10–20 years ago [24,25]. Short pulse visible and uv lasers operate now in similar $I\lambda^2$ regimes. The use of $K\alpha$ radiation to measure the electron energy distribution function and target preheating [26–28], resonance absorption and the role of density profile steepening by photon and electron momentum transfer [29,30], suprathermal electron energy deposition mechanisms [31,32], and demonstration of highly energetic electron production [33] have already been studied.

Similarly to what has been observed in the long pulse and long wavelength laser regime, it has been shown that laser absorption, hot electron generation and x-ray $K\alpha$ brightness from short pulse laser-produced plasmas can be enhanced with p-polarized light at large angle of incidence [22,34–38]. High conversion into supra-keV electrons is achieved during the subpicosecond laser pulse duration because hot electrons are produced by nonlinear effects such as Brunel ("vacuum heating") [17] or resonance absorption [25,39]. With a corrugated or a rough target surface, coupling of the incident laser energy with surface plasmon modes [40] is made possible and the total laser absorption increases [41,42].

In the present experiment, we have controlled the roughness of the target surface by varying the amplified spontaneous emission (ASE) prepulse energy level [43]. Previous studies have shown the strong influence of a poor energy contrast ratio between the laser pedestal and the short pulse on the x-ray pulse duration in the soft x-ray range [44] and on conversion efficiency [12,45,46]. Rippling of the target surface [47] by ASE removes the p-polarized radiation requirement for resonance absorption. We note that we operate in a prepulse fluence range which is very much smaller than in a previous work [45]. Indeed, our Schlieren experiments [48] have shown that with our level of prepulse energy (less than 1 GW/cm^2 irradiance), the electron density gradient scale length at critical density *remains smaller than the laser wavelength.* Being produced by highly nonlinear effects, the fast electrons are thought to last no longer than the duration of the laser pulse. Up to now, the time duration of the thermal x-ray pulse has been found to be less than ≈ 2 ps, the ultimate resolution of ultrafast streak cameras [49–51]. This incoherent x-ray flash can have interesting

applications in the study of conformation change kinetics of biological molecules [52,53] or in photoionized x-ray laser schemes [44,54].

In this paper, the spectral bandwidth and absolute brightness of both electrons and x-rays generated from ultra bright 100 fs laser interaction with solid targets will be characterized. In Secs. II and III, we describe the experimental setup and the experimental results. The analysis of our data and the description of our Monte Carlo model for electron energy deposition is presented in Sec. IV. Section V gives absolute electron fluence and $K\alpha$ yield and we conclude in Sec. VI.

II. EXPERIMENTAL SETUP

In the experiment, a full width at half maximum (FWHM) 100 fs, 1.5 mJ laser pulse is provided by a colliding-pulse mode-locked oscillator followed by a series of dye amplifiers (620 nm wavelength) pumped at a repetition rate of 10 Hz by a diode-injected, frequency-doubled, Q-switched Nd:YAG laser. Using a $f/8$ lens positioned at an angle of 7° with respect to normal incidence, we obtain a maximum focused intensity of 3×10^{16} W/cm^2 on target in a near diffraction-limited focal spot. The full width at half maximum (FWHM) spot size was measured to be 7 μm (Airy focus with the first null at a diameter of 12 μm) by equivalent focal plane microscopy. This corresponds roughly to a 50 μm^2 (FWHM) focal spot area. The laser pulse shape was measured during each experiment by a time-sampling third-order autocorrelator with a dynamic range larger than 10^5.

Due to the critical dependence of the x-ray emission on the ASE prepulse energy and prepulse onset delay [43] the characteristics of the ASE pedestal were monitored, with a resolution of 100 ps, by a 7 GHz oscilloscope and a fast photodiode. An ultrafast shutter consisting of a self-phase modulation water cell and a diffraction grating was added in front of the photodiode to reduce the short pulse intensity in the clear aperture of the diode thus avoiding high voltage distortions in the diode-oscilloscope combination. The delay of the onset of the prepulse with respect to the main pulse and the prepulse energy can be varied [45] by modifying the operating conditions of the Nd:YAG pump laser. Maximum x-ray conversion, monitored by a filtered ($h\nu>1$ keV) x-ray photodiode, was reached for an ASE fluence of 0.7 J/cm^2 [43]. This is close to the known damage threshold of aluminum. We note that our ASE pedestal intensity was smaller, *by more than one order of magnitude,* than the one used in a similar study by Cobble and co-workers [45] who used 650 fs, 248 nm laser pulses. No evidence was found for a variation of the absorbed laser energy with the polarization state of the laser. We note again that Schlieren measurements [48] show that the critical density surface of the ASE performed plasma is located at less than 1 μm (our spatial resolution) from the solid target surface at the time of laser peak.

To measure the laser energy penetration depth [26,55], we used bilayered targets consisting of different film thickness of aluminum deposited on SiO_2 and CaF_2 substrates. They were mounted on a X-Y motorized translation system in order to expose a fresh surface of the target to each laser shot. X-ray lines from the two layers of the target were collected at the same time by a double crystal VonHamos spectrograph built with two curved crystals positioned side by side. PET (pentaerythritol, $2d=8.742$ Å) or LiF (lithium fluoride, $2d=4.027$ Å) crystals, having both a 10 cm curvature radius, focused the x-ray lines on a film detector (Kodak SB392) covered by a 25 μm Be filter. The film density was converted to intensity by using the known crystal reflectivity, the filter transmission and the spectrograph geometry. To decrease the background on the film (which was attributed to high energy electron-induced x-ray fluorescence from the crystals) and to increase the resolution of the spectrograph, we have fitted the entrance port of the spectrograph with a permanent magnet producing a static magnetic field of 500 Gauss parallel to the film plane. The whole experimental setup was carefully designed to ensure a very good reproductibility of successive experiments which require a large number of shots (5000) and a systematic variation of the aluminum film thickness.

III. EXPERIMENTAL RESULTS

X-ray lines measured by the two PET crystals are shown in Fig. 1 using an aluminum film of 500 Å deposited on a fused silicate substrate. The laser intensity was 3×10^{16} W/cm^2. At energies close to 1580 eV (left in Fig.

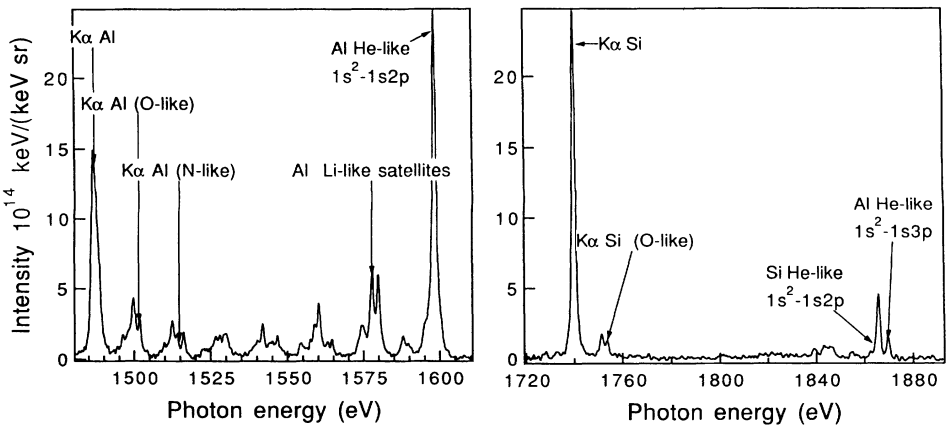

FIG. 1. Spectra obtained with 500 Å Al thickness on a SiO_2 substrate at a laser intensity of 3×10^{16} W/cm^2. Left: emission from aluminum plasma. Right: emission from silicon plasma.

1) well-defined x-ray line features correspond to a high temperature aluminum plasma from which the He-like $1s^2$-$1s2p$ resonance line and its lithiumlike dielectronic satellites are emitted. Based on the fact that we do not observe the H-like $1s$-$2p$ resonance line, RATION and SPECTRA computer code calculations [56], taking into account self absorption of the He-like $1s^2$-$1s2p$ resonance line, give an estimate of the electron temperature to be in the 150–250 eV range. From the spectral broadening of the dielectronic satellites, the density of the plasma has been evaluated [57] to be about 10^{23} cm^3. Weak emission from the heliumlike $1s^2$-$1s2p$ resonance line of silicon and blended emission from the heliumlike $1s^2$-$1s3p$ resonance line of aluminum can be seen in the right part of Fig. 1. Characteristic $1s^2$-$1s2p$ emission from the thermal plasma can be observed up to 2500 Å inside the target, in agreement with other results [55] as shown in Fig. 2. The apparent saturation of the line intensity at depths larger than 2500 Å is due to the limited penetration depth of thermal energy inside the target and to the increasing effect of autoabsorption with film thickness. Returning to Fig. 1, at energies close to 1500 eV, we observe both the $K\alpha$ line from "cold" aluminum (Al^{0+} to Al^{4+} transitions are blended) and shifted $K\alpha$ lines from Al^{5+} to Al^{9+}. These lines are the signature [26,58] of a low temperature plasma (< 50 eV) produced by the heating effect of the energetic electrons penetrating the target. The measured "cold" $K\alpha$ yield is far too high to be induced by the kilovolt radiation from the plasma.

Figure 3 shows the variation of the "cold" $K\alpha$ line (filled diamonds) intensity together with the Al^{5+} (open diamonds) and Si^{6+} (open circles) line intensities as a function of aluminum thickness. The saturation depth of the $K\alpha$ lines is now 10 000 Å compared to 2500 Å for the heliumlike $1s^2$-$1s2p$ resonance line. Monoenergetic electron beam excitation of these lines would correspond to a maximum electron energy of 16 keV [59,60]. Of course, we may expect a wide distribution of electron energies in the plasma. Saturation in Fig. 3 comes from the fact that the hot electrons do not create enough ionization in the deepest parts of the target to compensate for autoabsorption (in the case of $K\alpha$ Al) or reabsorbtion (in the case of

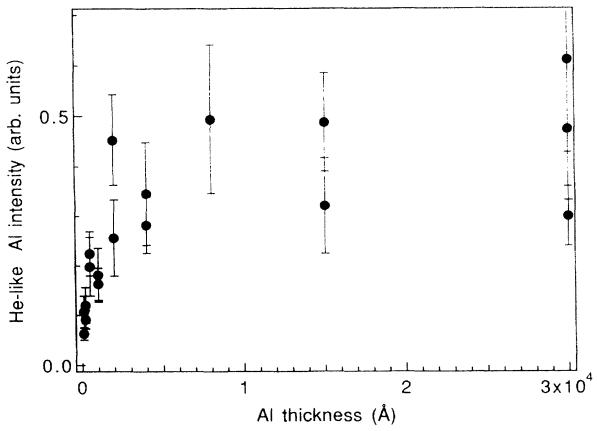

FIG. 2. He-like $1s^2$-$1s2p$ resonance line intensity as a function of Al thickness at a laser intensity of 3×10^{16} W/cm^2.

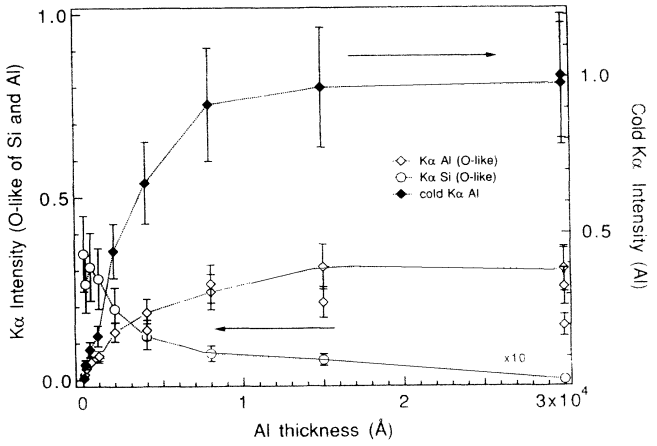

FIG. 3. "Cold" $K\alpha$ line of Al and oxygenlike $K\alpha$ of Al and Si as a function of Al thickness. Filled diamonds (right scale): Al "cold" $K\alpha$. Open diamonds (left scale): Al O-like $K\alpha$. Open circles (left scale): Si O-like $K\alpha$. Lines are drawn as an aid to the eye.

$K\alpha$ Si). From Fig. 3 one can see also that the hot electron heating depths deduced from the variation with Al thickness of the "cold" $K\alpha$ emission and of the Al^{5+} and Si^{6+} emissions are almost the same. This is because energetic electrons deposited most of their initial energy close to their mean penetration depth. We note that the target region heated indirectly by hot electron energy deposition is, according to our measurements, sufficiently inside the target to be unperturbed by thermal conduction heating from the thermal plasma [7].

IV. MONTE CARLO ANALYSIS OF THE ELECTRON DISTRIBUTION FUNCTION

The electron energy distribution has been unfolded from experiment with the help of Monte Carlo simulations of the electron energy penetration and deposition inside the target [61–66]. The energy release of the electron beam can be converted to material temperature through the known equation of state. Assuming local thermodynamic equilibrium (LTE) to be valid in the bulk of the target, we can obtain the spatial profile of both the "cold" $K\alpha$ and Al^{5+} and Si^{6+} intensities for different shapes of the electron energy distribution function.

We have analyzed our experimental data with a Monte Carlo calculation in multilayered and multimaterial solid targets. The code follows the 3D trajectories of a single electron interacting with the target through elastic (screened Rutherford cross sections) and inelastic (Bethe stopping power cross sections) scattering. By weighting the results obtained at several electron energies, we can predict the penetration characteristics of a more complex electron distribution function. This is quite useful because hot electrons are generated in the expanding plasma where low electron densities do not insure an isotropic, Maxwellian electron energy distribution [67]. Fluorescence efficiencies incorporating Auger decay branching ratios have been used to calculate the $K\alpha$ line emission at different target depths. The optical depth

from the emitting point to the target surface is taken into account. The influence of opacity effects on the $K\alpha$ radiation escaping the plasma is particularly significant for Al-SiO_2 targets because the emission from Si is strongly absorbed by the Al K edge. The energy deposition is evaluated as a function of position inside the target. The temperature rise is calculated using the quotidian equation of state (QEOS) which is well suited to high density plasmas [68]. A simple LTE calculation, with ionization lowering adjusted to reproduce the finite $Z=2.7$ ionization of solid aluminum at low temperatures, has been used to calculate the relative intensities of the $K\alpha$ lines from ions between Al^{5+} and Al^{10+} (the corresponding lines can be seen in Fig. 1).

The overall efficiency of our $K\alpha$ x-ray diagnostic system, including the Monte Carlo code predictions and the VonHamos spectrograph and film detector was absolutely calibrated using a monoenergetic electron beam as a $K\alpha$ source. A 20 keV electron beam with an average power between 100 and 1000 W has been focused in a 1 mm focal spot onto pure aluminum, Al-SiO_2 and Al-CaF_2 targets. Our spectrograph was placed in a position similar to the one used in the laser experiment. X-ray diode absolute measurements of the resulting $K\alpha$ x-ray emission have been compared to the VonHamos spectrograph and film response and to the predicted Monte Carlo $K\alpha$ emission. The absolute intensity measurements were found to be within a factor of two of the values determined from the known crystal reflectivity and spectrograph geometry. The measured variation of the $K\alpha$ intensity as a function of the electron beam fluence was also found in very good agreement with the Monte Carlo model predictions.

The hot electron distribution function depends on the laser intensity and on the nature of the outside layer material—here aluminum. To check the consistency of our results, we have made measurements with both CaF_2 and SiO_2 substrates. The electron distribution function was determined form the shape of the ratio of Si to Al and Ca to Al "cold" $K\alpha$ lines as a function of the aluminum film thickness. Results for the CaF_2 substrate are shown in Fig. 4. This substrate is found particularly useful for high energy electrons (>10 keV) and large Al thicknesses (above 10 000 Å) because Ca $K\alpha$ radiation is only weakly reabsorbed through the Al layer. Experimental data is well fitted by monoenergetic electron contributions at 3, 8, 16, 28, and 50 keV with corresponding weight factors in energy of 21%, 47%, 23%, 6.9%, and 2.1%. To better show the significance of this fit, the curves labeled (a,b,c) in Fig. 4 give the successive contributions to the fit of $\{3,8,16,0,0\}$ keV electrons (a), of $\{3,8,16,28,0\}$ keV electrons (b), and of $\{3,8,16,28,50\}$ keV electrons (c). The same distribution applied to the case of the SiO_2 substrate is shown in Fig. 5. One can see the excellent consistency of the two data sets shown in Figs. 4 and 5.

The corresponding energy distribution is shown in Fig. 6 with filled circles. To double check the validity of our data analysis, we have changed the $\{3,8,16,28,50\}$ keV electron energy groups to another set of energy groups, namely $\{3,6,10,20,40\}$ keV. Results shown with triangles in Fig. 6 agree very well with those obtained with the initial set of electron energies. The data points can be fitted with an exponential function having a slope corresponding to an electron "temperature" of 8.5 keV. However, we cannot tell the exact distribution at electron energies larger than 50 keV which may be responsible for the slight discrepancy of the $K\alpha$ line ratio for Al (see Fig. 5) at large depths. Within experimental uncertainty, our hot electron "temperature" result is slightly lower than the one predicted by available absorption resonance theories by Estabrook and Kruer [69] and Burnett and his co-workers [27] for intensities in the $1-3\times10^{16}$ W/cm^2 range, respectively, (9.8–15 keV) and (8.4–12 keV). It is in better agreement with Gibbon and Bell's particle in cell simulations [70].

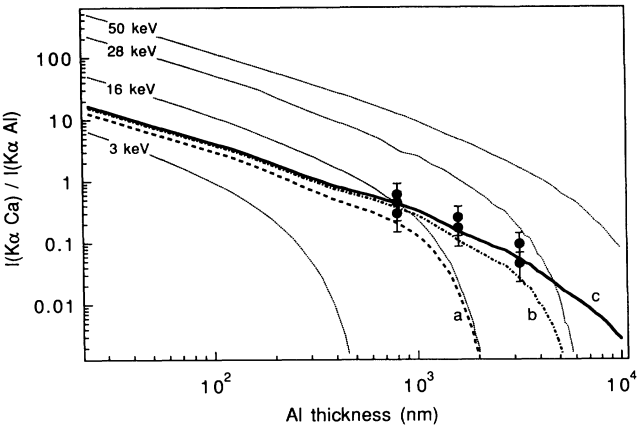

FIG. 4. Ratio of the intensities of "cold" $K\alpha$ lines of Ca and Al as a function of Al thickness. The solid curve is the calculated ratio for the electron distribution function giving the best fit. Curves a, b, c show the different contributions of electron energies above 28 keV (see text). Dotted curves are monoenergetic electron contributions at different energies. Filled points are the experimental results.

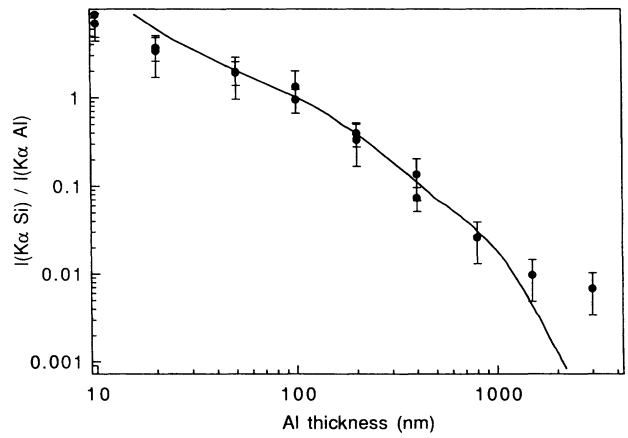

FIG. 5. Ratio of the intensities of the $K\alpha$ lines of Si and Al as a function of Al thickness. The solid curve is the ratio calculated with *the same* distribution function as the one used in Fig. 4.

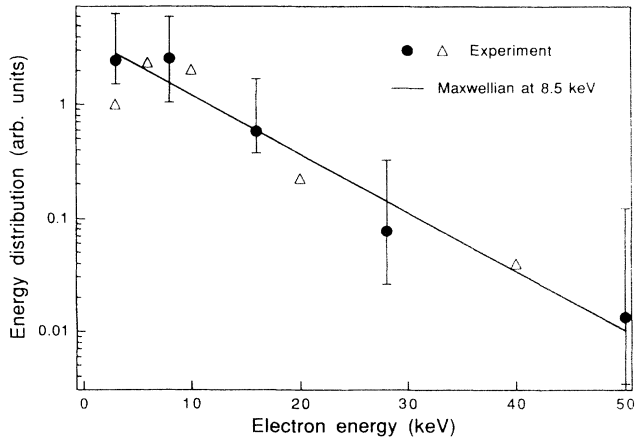

FIG. 6. Electron energy distribution function as a function of electron energy. Dots: obtained with energy groups (3, 8, 16, 28, 50) keV. Triangles: obtained with energy groups (3, 6, 10, 20, 40) keV. The solid line is the best exponential fit with an inverse slope of 8.5 keV.

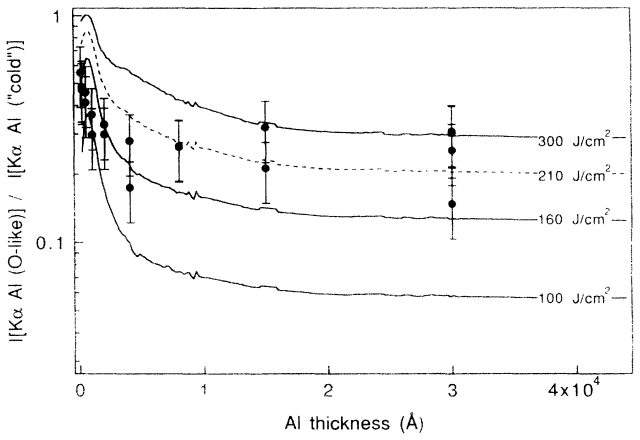

FIG. 7. Ratio of the intensities of O-like to "cold" al $K\alpha$ lines as a function of Al thickness. Dots: experimental results obtained at 3×10^{16} W/cm^2. The lines are the Monte Carlo results for different electron fluences. The best fit is obtained for 210 J/cm^2 (dashed line).

V. HOT ELECTRON FLUENCE AND $K\alpha$ YIELD

A direct comparison of the absolutely measured "cold" Al $K\alpha$ line intensity with our Monte Carlo predictions gives an estimate of 12 ± 5 % for the conversion efficiency of incident laser energy into hot electron energy. We note that the laser absorption has been determined to be 25 ± 10 % by specular reflection and scattering measurements [43]. However, a quantitative description of hot electron deposition requires the absolute measurement of the electron fluence which we define as the ratio of the total electron energy incident on target to the deposition area. We have used two different methods to measure this quantity.

First, the hot electron fluence can be deduced from an evaluation of the preheat temperature of the target. This can be done by measuring the ratio of the oxygenlike Al^{5+} $K\alpha$ line to the "cold" Al^{0+}-Al^{4+} $K\alpha$ line as a function of Al thickness at constant laser intensity. Using the Monte Carlo simulations coupled to the LTE ionization predictions we have determined the spatial dependence of the charge state distribution inside the target. In these calculations, we have used the hot electron distribution of Fig. 6 and we have assumed that this distribution did not change with the aluminum thickness. Using the incident electron fluence as a parameter, we have calculated the ratio of the Al^{5+} to the "cold" $K\alpha$ lines and we have adjusted the calculated results to the experiment. However, the Monte Carlo code takes into account the energy deposited by hot electrons solely. Accordingly, experiments should give less oxygenlike $K\alpha$ at depths smaller than 2500 Å (see Figs. 2 and 3) where the temperature rise is governed by thermal conduction rather than by hot electron deposition. This is shown in Fig. 7 which gives the oxygenlike to "cold" $K\alpha$ line ratio as a function of Al thickness. Monte Carlo predictions with the hot electron fluence as a parameter are also shown for comparison. Above 10 000 Å, the $K\alpha$ ratio is independent of aluminum thickness, as expected; we can deduce an electron fluence of 210 ± 50 J/cm^2. The corresponding calculated hot electron preheat temperature is 20–30 eV.

A second method of determining the electron fluence requires a measurement of the $K\alpha$ emission spot size. This was done by using a knife edge technique [71]. Spatial resolution better than 2 μm and a very good signal-to-noise ratio, as compared to the one obtained in standard pinhole imaging, were found very useful in our case. To accommodate the small number of x-ray photons at each shot, we replaced the film detector by a cooled (-40° C) x-ray sensitive charge-coupled device (CCD) detector placed at 20° from target normal. This allows ≈ 50 eV spectral resolution of the incident photons by using single photon counting techniques [72]. This spectral resolution was sufficient to isolate the $K\alpha$ line from the emission of the thermal plasma. After deconvolution of the knife edge results by a simple derivation [71], we obtain the image of the spectrally resolved $K\alpha$ line of Fig. 8.

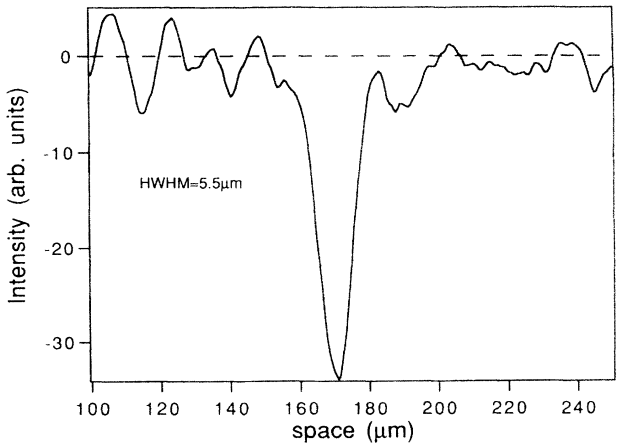

FIG. 8. Intensity profile of the Al $K\alpha$ spot size measured by the knife-edge technique. Laser intensity is 1.5×10^{16} W/cm^2. The diameter is 11 μm compared to 8 μm for the visible laser.

This corresponds to an emitting surface of 95 ± 20 μm^2, slightly larger than the visible focal spot. Previous results obtained in the long pulse (600 ps) regime [73,74] show much larger lateral electron transport distances. The corresponding electron fluence deduced from the 1.5 mJ laser energy and the 12.5% conversion efficiency is 197 J/cm^2, in very good agreement with the value obtained from the target preheat measurement. Combined with the known $K\alpha$ production efficiency for 8 keV electrons in aluminum, we obtained an x-ray fluence of ~ 0.5 J/cm^2.

Scaling laws that predict the variation of the thermal plasma x-ray yield as the laser and target parameters are varied have been proposed [16]. For $K\alpha$ emission, the physical situation is quite different because the mechanism governing the x-ray yield is hot electron production [36]. We have measured and calculated the conversion efficiency of electron energy into $K\alpha$ photons for several target materials. Results are summarized in Fig. 9 which gives a comparison of the $K\alpha$ yield obtained from the experimental CCD results and from the Monte Carlo calculations. The $K\alpha$ yield is expressed as the number of photons emitted per steradian for our laser intensity of 1.5 mJ. Reabsorption effects (see the dashed line in Fig. 9) reduce the $K\alpha$ yield for low Z materials. In the Monte Carlo calculations, we have assumed that the incident electron energy distribution function (see Fig. 6) was the same for all the elements.

The measured conversion efficiency into one line, in a bandwidth $\lambda/\delta\lambda = 1000$ (0.1% BW) is 0.02%. This value is comparable to the measured conversion efficiency of thermal plasma lines (e.g., He-like resonance lines) in the 1.5 keV range [75,76] but is smaller than the one reached with foam or structured targets [42]. Regarding the x-ray pulse duration, we note that thermal emission has been shown to be lengthened when a prepulse was used; our x-ray generation process is completely different since it relies on suprathermal electron production which occurs only during the driving laser pulse. Converted to spectral brightness units [photons/(s mrad^2 mm^2 0.1% BW)] the femtosecond $K\alpha$ x-ray source yield is still higher than, e.g., the projected European Synchrotron Radiation Facility undulator yield [77] which is limited to pulse durations of several tenths of picoseconds.

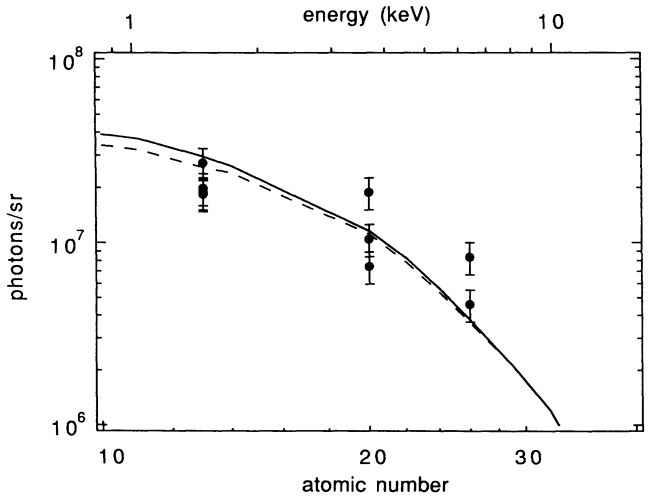

FIG. 9. Number of $K\alpha$ photons emitted per steradian as a function of the target substrate material. The upper scale gives the corresponding photon energy. Solid line: Monte Carlo calculations without reabsorption effects. Dashed line: with reabsorption effects.

VI. DISCUSSION AND CONCLUSIONS

We have characterized the hot electron pulse emitted by an ultrashort (100 fs) and bright (3×10^{16} W/cm^2) laser pulse on multilayered solid targets. The resulting $K\alpha$ yield is 2.5×10^7 photons/sr pulse for aluminum at 1.5 keV. Using Monte Carlo calculations to analyze the results, we have found that the electron distribution function can be fitted by a 8.5 keV Maxwellian function. This is in good agreement with the hot electron "temperature" obtained from the theory of resonance absorption in short density scalelength plasmas and with particle in cell simulations of "vacuum heating." By measuring the relative intensity of the temperature-dependent shifted $K\alpha$ lines of Al, we have determined the hot electron preheat to be 20–30 eV and we have measured 12% conversion efficiency from laser energy into suprathermal electron energy. The measured size of the $K\alpha$ emission spot is comparable to the laser spot size.

We note the important effect of the ASE laser pedestal on the $K\alpha$ source output. At this time, theoretical understanding of the effect of the ASE prepulse is not complete. High intensity contrast experiments [22,36] have shown that resonance absorption plays a major role in p polarized, 60° incidence angle, 2×10^{16} W/cm^2 picosecond laser interaction. Our results are not very different regarding the hot electron conversion efficiency and hot electron "temperature" despite the factor of 10 in laser pulse duration. Particle-in-cell (PIC) simulations are in progress to understand the interplay of vacuum heating and resonance absorption processes in the hot electron production mechanisms [78]. Two-dimensional PIC simulations will be necessary to study the effects of surface rippling on laser absorption.

This paper demonstrates that the control of the target roughness by surface melting with a mild, close to damage threshold, laser prepulse is a very powerful alternative to the use of corrugated targets (gratinglike) or the use of a low density foam for short pulse x-ray production, stability, and quasimonochromatic hard x-ray flash production. Assuming that the duration of the hot electron pulse is no longer than the visible laser pulse, the hot electron current density is about 2.5×10^5 MA/cm^2. The $K\alpha$ time duration should not be very different from the electron pulse duration. In fact, the thermalization time of 8 keV electrons is about 15 fs, according to Monte Carlo estimates. The hot electron "temperature" being determined by the nature of the outer layer material and laser intensity, specially designed bilayered targets of a

low-Z "electron convertor" and a much higher-Z "x-ray generator" can be used. We have demonstrated that the scaling to much higher energies than the Al $K\alpha$ (1.5 keV) was possible. For the Ca $K\alpha$ at 3.7 keV and Fe $K\alpha$ at 6.4 keV we have measured a photon yield close to 10^7 photons/sr pulse.

ACKNOWLEDGMENTS

We thank R. Mancini for helpful discussions and J. Delettrez for particle-in-cell calculations. This work was partly supported by a Direction de Recherches et Eudes Techniques Grant No. 90/057.

[1] M. M. Murnane, H. C. Kaypten, M. D. Rosen, and R. W. Falcone, Science **251**, 531 (1991).

[2] D. Kuhlke, U. Herpes, and D. v. d. Linde, Appl. Phys. Lett. **50**, 1785 (1987).

[3] O. L. Landen, M. Campbell, and M. D. Perry, Opt. Commun. **63**, 253 (1987).

[4] H. M. Milchberg, R. R. Freeman, and S. C. Davey, Phys. Rev. Lett. **61**, 2364 (1988).

[5] D. G. Stearns, O. L. Landen, E. M. Campbell, and J. H. Scofield, Phys. Rev. **37**, 1684 (1988).

[6] M. M. Murnane, H. C. Kaypten, and R. W. Falcone, Phys. Rev. Lett. **62**, 155 (1989).

[7] P. Audebert, J. P. Geindre, J. C. Gauthier, A. Mysyrowicz, J. P. Chambaret, and A. Antonetti, Europhys. Lett. **19**, 189 (1992).

[8] J. C. Kieffer, M. Chaker, J. P. Matte, H. Pépin, Y. Coté, Y. Beaudoin, T. W. Johnston, C. Y. Chien, S. Coe, G. Mourou, and O. Peyrusse, Phys. Fluids B **5**, 2330 (1993).

[9] J. A. Cobble, G. A. Kyrala, A. A. Hauer, A. J. Taylor, C. C. Gomez, N. Delamater, and G. T. Schappert, Phys. Rev. A **39**, 454 (1989).

[10] W. Rozmus and V. T. Tikhonchuk, Phys. Rev. A **42**, 7401 (1990).

[11] W. Rozmus and V. T. Tikhonchuk, Phys. Rev. A **46**, 7810 (1992).

[12] O. Willi, G. Kiehn, J. Edwards, V. Barrow, R. A. Smith, J. Wark, and E. Turcu, Europhys. Lett. **10**, 141 (1989).

[13] D. Riley, L. A. Gizzi, F. Y. Khattak, A. J. Mackinnon, S. M. Vaina, and O. Willi, Phys. Rev. Lett. **69**, 3729 (1992).

[14] H. M. Milchberg, I. Lyubomirsky, and C. G. Durfee III, Phys. Rev. Lett. **67**, 2564 (1991).

[15] J. Denavit, Phys. Rev. Lett. **69**, 3052 (1992).

[16] M. Rosen, SPIE Proc. **1229**, 160 (1990).

[17] F. Brunel, Phys. Rev. Lett. **59**, 52 (1987).

[18] F. Brunel, Phys. Fluids **31**, 2714 (1988).

[19] G. Bonnaud, P. Gibbon, J. Kindel, and E. Williams, Laser Part. Beams **9**, 339 (1991).

[20] E. Gamaly, Phys. Fluids B **5**, 3765 (1993).

[21] B. N. Chichkov, Y. Kato, and M. Murakami, Phys. Rev. A **46**, 4512 (1992).

[22] D. D. Meyerhofer, H. Chen, J. A. Delettrez, B. Soom, S. Uchida, and B. Yaakobi, Phys. Fluids B **5**, 2584 (1993).

[23] A. Rousse, F. Falliès, J. P. Geindre, P. P. Audebert, J. C. Gauthier, A. Mysyrowicz, G. Grillon, J. P. Chambaret, and A. Antonetti, OSA Proceedings on *Short Wavelength V: Physics with Intense Laser Pulses,* edited by M. D. Perry and P. Corkum (Optical Society of America, Washington, DC, 1993), Vol. 17, pp. 185–189.

[24] A. Rubenchick and S. Witkowski, *Handbook of Plasma Physics: Physics of Laser Plasmas* (Elsevier, Amsterdam, 1991), Vol. 3.

[25] W. L. Kruer, *The Physics of Laser Plasma Interactions* (Addison-Wesley, Redwood City, 1988), Vol. 73.

[26] J. Hares, J. Kilkenny, M. M. Key, and J. G. Lunney, Phys. Rev. Lett. **42**, 1216 (1979).

[27] N. H. Burnett, G. D. Enright, A. Avery, A. Loen, and J. C. Kieffer, Phys. Rev. A **29**, 2294 (1984).

[28] E. M. Campbell, Phys. Fluids B **4**, 3781 (1992).

[29] D. W. Forslund, J. M. Kindel, and K. Lee, Phys. Rev. Lett. **39**, 284 (1977).

[30] J. R. Albritton and A. B. Langdon, Phys. Rev. Lett. **45**, 1794 (1980).

[31] K. A. Brueckner, Phys. Rev. Lett. **36**, 677 (1976).

[32] R. J. Harrach and R. E. Kidder, Phys. Rev. A **23**, 887 (1981).

[33] G. D. Enright, Phys. Rev. A **32**, 3578 (1985).

[34] J. C. Kieffer, P. Audebert, M. Chaker, J. P. Matte, H. Pépin, T. W. Johnston, P. Maine, D. Meyerhofer, J. Delettrez, D. Strickland, P. Bado, and G. Mourou, Phys. Rev. Lett. **62**, 760 (1989).

[35] R. Fedosejevs, R. Ottmann, R. Sigel, G. Kühnle, S. Szatmari, and F. P. Schäfer, Appl. Phys. B **50**, 79 (1990).

[36] H. Chen, B. Soon, B. Yaakobi, S. Uchida, and D. Meyerhofer, Phys. Rev. Lett. **70**, 3431 (1993).

[37] U. Teubner, J. Bergmann, B. v. Wonterghem, F. P. Schäfer, and R. Sauerbrey, Phys. Rev. Lett. **70**, 794 (1993).

[38] M. Schnürer, P. V. Nickles, M. P. Kalashnikov, F. Bilhardt, A. Y. Faenov, and B. A. Brunetkin, SPIE Proc. **2015**, 261 (1993).

[39] H. Maki and K. Niu, J. Phys. Soc. Jpn. **45**, 269 (1978).

[40] R. Dragila and E. G. Gamaly, Phys. Rev. A **44**, 6828 (1991).

[41] S. P. Gordon, R. Sheppard, T. Donelly, D. Price, B. White, A. Osterheld, H. Hamster, A. Sullivan, and R. W. Falcone, OSA Proceedings on *Short Wavelength V: Physcis with Intense Laser Pulses,* edited by M. D. Perry and P. Corkum (Optical Society of America, Washington, DC, 1993), Vol. 17, pp. 203–206.

[42] S. P. Gordon, T. Donnelly, A. Sullivan, H. Hamster, and R. W. Falcone, Opt. Lett. **19**, 7 (1994).

[43] P. Audebert, J. P. Geindre, J. C. Gauthier, R. Benattar, J. P. Chambaret, A. Mysyrowicz, and A. Antonetti, in Atomic Processes in Plasmas, edited by E. S. Marmar and J. L. Terry AIP Conf. Proc. No. 257 (AIP, New York, 1991), p. 58.

[44] M. M. Murnane, H. C. Kapteyn, and R. W. Falcone, IEEE J. Quantum Electron. **25**, 2417 (1989).

[45] J. A. Cobble, G. T. Schappert, L. A. Jones, A. J. Taylor, G. A. Kyrala, and R. D. Fulton, J. Appl. Phys. **69**, 3369 (1991).

[46] U. Teubner, G. Kühnle, and F. P. Schäfer, Appl. Phys. B **54**, 493 (1992).

[47] J. C. Koo and R. E. Slusher, Appl. Phys. Lett. **28**, 814 (1976).

[48] R. Benattar, J. P. Geindre, P. Audebert, J. C. Gauthier, J. P. Chambaret, A. Mysyrowicz, and A. Antonetti, Opt. Commun. **88**, 376 (1992).

[49] M. M. Murnane, H. C. Kapteyn, and R. W. Falcone,

Appl. Phys. Lett. **56**, 1948 (1990).
[50] J. C. Kieffer, Y. Beaudoin, M. Chaker, C. Y. Coté, and H. Pépin, in *X-ray Lasers,* edited by E. E. Fill, IOP Conf. Proc. No. 125 (Institute of Physics and Physical Society, London, 1992), p. 201.
[51] A. Mens, R. Sauneuf, P. Schirman, R. Verrecchia, P. Audebert, J. C. Gauthier, J. P. Geindre, A. Antonetti, J. P. Chambaret, G. Hamoniaux, and A. Mysyrowicz, *UltraFast Phenomena VIII* (Springer-Verlag, Berlin, 1992), Vol. 55, p. 147.
[52] M. J. Rosker, F. W. Wise, and C. L. Tang, Phys. Rev. Lett. **57**, 321 (1986).
[53] T. Teng, H. W. Huang, and G. A. Olah, Biochemsitry **26**, 8066 (1987).
[54] D. C. Eder, P. Amendt, and S. C. Wilks, Phys. Rev. A **45**, 6761 (1992).
[55] A. Zigler, P. G. Burkhalter, D. J. Nagel, M. D. Rosen, K. Boyer, G. Gibson, T. S. Luk, A. McPherson, and C. K. Rhodes, Appl. Phys. Lett. **59**, 534 (1991).
[56] R. W. Lee, B. L. Whitten and R. E. Strout, J. Quant. Spectros. Radiat. Transfer **32**, 91 (1985).
[57] R. C. Mancini, P. Audebert, J. P. Geindre, A. Rousse, F. Falliès, J. C. Gauthier, A. Mysyrowicz, J. P. Chambaret, and A. Antonetti, J. Phys. B **27**, 1671 (1994).
[58] A. Hauer, W. Priedhorsky, and D. v. Hulsteyn, Appl. Opt. **20**, 3477 (1981).
[59] I. V. Spencer, Phys. Rev. **98**, 1597 (1955).
[60] T. E. Everhart and P. H. Hoff, J. Appl. Phys. **42**, 5837 (1971).
[61] M. Inokuti, Rev. Mod. Phys. **43**, 3 (1971).
[62] M. Inokuti, J. L. Dehmer, T. Baer, and J. D. Hanson, Phys. Rev. A **23**, 1 (1981).
[63] S. Ichimura and R. Shimizu, Surf. Sci. **112**, 386 (1981).
[64] R. J. Mason, Phys. Rev. Lett. **47**, 652 (1981).
[65] L. Reimer, *Transmission Electron Microscopy* (Springer-Verlag, Berlin 1984).
[66] R. F. Egerton, *Electron Energy Loss Spectroscopy* (Plenum, New York, 1986).
[67] J. C. Kieffer, J. P. Matte, M. Chaker, Y. Beaudoin, C. Y. Chien, G. Mourou, J. Dubau, and M. K. Inal, Phys. Rev. Lett. **68**, 480 (1992).
[68] R. M. More, K. H. Warren, D. A. Young, and G. B. Zimmerman, Phys. Fluids **31**, 3059 (1988).
[69] K. Estabrook and W. L. Kruer, Phys. Rev. Lett. **40**, 42 (1978).
[70] P. Gibbon and A. R. Bell (private communication).
[71] P. Alaterre, C. Popovics, J. P. Geindre, and J. C. Gauthier, Opt. Commun. **49**, 140 (1984).
[72] E. G. Chowanietz, D. H. Lumb, and A. A. Wells, SPIE Proc. **587**, 38 (1985).
[73] J. C. Kieffer, H. Pépin, and F. Amiranoff, Appl. Phys. Lett. **44**, 494 (1984).
[74] F. Amiranoff, Ph.D. thesis, University Paris–Sud, 1984.
[75] I. C. E. Turcu, I. N. Ross, P. Trenda, C. W. Wharton, R. A. Meldrum, H. Daido, M. S. Schulz, P. Fluck, A. G. Michette, A. P. Juna, J. R. Maldonado, H. Shields, G. J. Tallents, L. Dwivedi, J. Krishnan, D. L. Stevens, T. J. Jenner, D. Batani, and H. Goodson, SPIE Proc. **2015**, 243 (1993).
[76] M. M. Murnane, H. C. Kaypten, S. P. Gordon, J. Bokor, E. N. Glytsis, and R. W. Falcone, Appl. Phys. Lett. **62**, 1068 (1993).
[77] I. Nenner and A. Lompré (private communication).
[78] J. Delettrez, Laboratory for Laser Energetics LLE Review 58, NTIS document No. DOE/SF/19460-7, 1994 (unpublished), p. 76.